IAC-11-A6.1.03

RESULTS OF OPTICAL SURVEYS FOR SPACE DEBRIS IN MEO

T. Schildknecht

Astronomical Institute, University of Bern, CH-3012 Bern, Switzerland
thomas.schildknecht@aiub.unibe.ch

A. Vananti [1], A. Hinze[1], J. Herzog[1], H. Krag[2]

[1]Astronomical Institute, University of Bern, CH-3012 Bern, Switzerland
[2]ESA ESOC, Robert-Bosch-Strasse 5, 64293 Darmstadt, Germany

During the last decades considerable effort has been spent to measure the space debris environment in different orbital regimes using radar and optical sensors. Most surveys concentrated either on the densely populated low Earth orbit altitudes (LEO) or on the unique region of the geostationary ring (GEO). Some limited results from surveys of the geostationary transfer region (GTO) are available, as well. The increasingly populated medium Earth Orbit (MEO) space used by the global navigation satellite constellations like GPS, GLONASS, Beidou-2/COMPASS, and GALILEO has not been systematically investigated so far.

Previous GEO surveys revealed a substantial number of small-size debris, leading space debris modelers to assume a number of at least 10 breakup events in the GEO region (including the two known events). Applying the same ratio of fragmentations per inserted object to approximately 230 MEO catalogue objects would lead to a high probability for one or several breakup events in the MEO region. Measurements to characterize the debris environment in MEO are thus highly desirable.

Dedicated MEO survey strategies were developed and corresponding survey campaigns performed at the ESA 1-meter telescope in Tenerife. The paper presents the results from these surveys and analyzes their statistical significance. Upper limits for the number of breakup events in different orbital planes are derived based on a simulated breakup event population.

I. INTRODUCTION

Systematic surveys of the geostationary ring (GEO) and the geostationary transfer orbit environment (GTO) revealed a considerable population of small-size space debris in these regions. The type of this debris ranges from mission-related debris like instrument and cooler covers to breakup fragments and finally high area-to-mass ratio debris which is either the results from breakup events or from aging processes acting on spacecraft outer surfaces [1].

The observed space debris population in GEO lead space debris modelers to assume a number of at least 10 breakup events in this region (including the two known events) [2]. Applying the same ratio of fragmentations per inserted object (weighted by the number of years in orbit) to the approximately 230 catalogue objects in the current navigation satellite constellations in medium Earth orbit (MEO) leads to a high probability for one or several breakup events in MEO.

No systematic investigation of the MEO region for small-size space debris has been conducted so far and ESA thus decided to extend its optical surveys from GEO and GTO to MEO. This required the development of observations scenarios for optical MEO surveys [3]. In order to study the performance of observation scenarios, a synthetic breakup population was generated (see Section II). This population was then also used to statistically analyze the observation results with the aim to exclude breakup events for certain regions (Section IV).

Experimental MEO observation campaigns were conducted with the 1-meter ESA Space Debris Telescope (ESASDT) on Tenerife during the year 2010.

II. EXPLOSION MODEL AND SYNTHETIC POPULATION

In order to identify possible debris clouds due to breakups in the MEO region, a set of fragmentations has been simulated, taking into account a reasonable range of ejection velocities as a function of the fragment size.

For the breakup model we refer to the study of Pardini and Anselmo [4]. Assuming debris of spherical shape and a total mass of 2500kg for the parent body, the cumulative number of fragments as a function of the diameter can be calculated (Figure 1 top). In the explosion model an isotropic ejection of the fragments was assumed. The velocity distribution is shown in Figure 1 bottom.

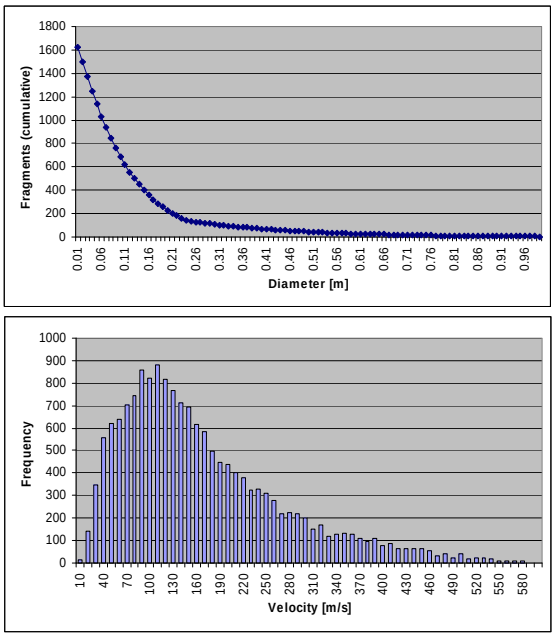

Figure 1: Cumulative number of fragments as a function of the diameter (top) and the distribution of the velocity of the fragments (bottom).

The culmination point and the ascending node were selected as representative locations along the orbit for the explosion. The choice of the location is relevant for the orbits of the fragments. Due to the explosion the orbit of the fragments will differ from the original orbit. Depending on the plane orientation change, either the right ascension of the ascending node Ω or the inclination *i* will show a larger variation. GPS and GLONASS orbits were taken into account and the distributions of the single orbital elements after the explosions were calculated. As a consequence of the explosion the distribution of the semi-major axis is broadened around the value of the original orbit with a standard deviation of about 1000km. All the fragments show a more eccentric orbit than the one of the parent object, with a broad range of values between 0.01 and 0.1 and a highest value of 0.03. The analysis of the inclination and the node showed that the fragmentation at the node is characterized by a narrow dispersion in Ω and a wide spreading in *i*. If the breakup event happens at the culmination point the situation for Ω and *i* is right the opposite. Furthermore the argument of perigee and, after few complete orbits, the mean anomaly, are homogeneously distributed. Since a fragmentation event can occur to each of the MEO objects in the reference catalogue, the next step consists in applying the explosion dispersion to the distribution of the reference population. The convolution of the two distributions was calculated for all orbital elements. In the eccentricity the dispersion due to the explosion is predominant, whereas for the ascending node the width is mostly characterized by the existing population distribution. The convoluted elements values have approximately a Gaussian distribution. Finally the evolution over time of the orbital elements was considered. We referred to the "Detailed assessment of a European Space Surveillance System" study [5]. In this study GPS and GLONASS orbits were propagated over several decades. The force model included lunisolar perturbations, Earth's potential up to degree and order 30, Earth tides, general relativity and the direct radiation pressure. JPL DE200 ephemeris data for Moon and Sun, the JGM3 model for the Earth potential, and the UTCSR ocean tide model were used. Taking the age of the satellites into account the explosion distribution was convoluted with the dispersion of the orbital elements after 15 years. Assuming that the deviations can be described with a Gaussian distribution, the resulting distribution can be characterized by a standard deviation, composed by the dispersion due to the explosion and the evolution: $\sigma^2_{tot} = \sigma^2_{expl} + \sigma^2_{evol}$.

Description	σ expl.	σ evol.	σ tot.
a [km]	1200	~ 0	1220
e	0.02	0.01	0.022
i [°]	1.5	0.5	1.6
Ω [°]	5	5	7

Table 1: Summary of the standard deviation in the orbital elements.

A synthetic population of 1000 objects was generated using Gaussian distributions with the total deviations and with the centers at the average orbital elements of different subgroups in the reference population. Figure 2 shows the poles of the orbit planes of the population in a gnomonic representation. A given observation field with a right ascension α and a declination δ is crossed by all orbits with inclinations *i* equal to or larger than $|\delta|$ and ascending node Ω that fulfill the equation:

$$\sin(\alpha - \Omega) = \tan(\delta)\cot(i). \quad (1)$$

In the (Ω, *i*)-space the latter equation defines a stripe of finite width depending on the field of view (FOV) of the optical sensor. In this representation the stripes are delimited by straight parallel lines. The covered field is identified with the normal to the stripe through the center of the diagram. The azimuth of the normal line and

the radius, from the center up to the stripe, are directly related to the (α, δ) field.

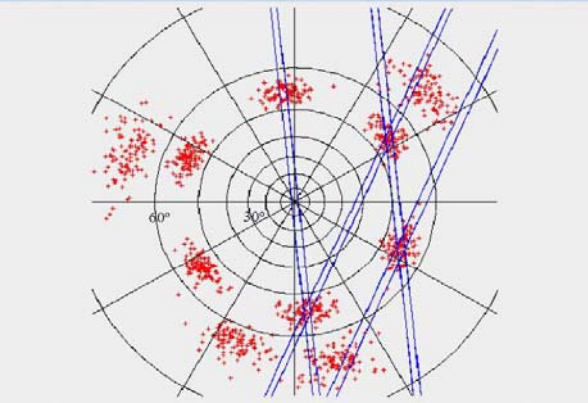

Figure 2: Poles of orbit planes of the synthetic population (gnomonic projection)

III. SURVEYS

The regions of interest for MEO debris surveys are obviously the orbital planes of the GPS and the GLONASS navigation satellite constellations. The satellites of the GPS constellation are arranged in six orbital planes (plus one additional plane of the "Block-I" test configuration) and GLONASS satellites are located in three orbital planes. Figure 3 shows the tracks of all known catalogue objects in GLONASS and GPS planes in a geocentric (α, δ) inertial system. Orbits in red are active satellites whereas black indicates non-active satellites. Depending on the season and on the preferred observation geometry only part of these orbital planes were observable by the ESASDT at a given time. The number of active and non-active satellites in these nine orbital planes is given in Table 2. The first row indicates the approximate right ascension of the ascending node Ω of the planes (January 2010) A typical inclination for GPS satellites is around 55° while GLONASS satellites have a typical inclinations of about 65°.

	GLONASS			GPS					
Group/plane	**G1**	**G2**	**G3**	**N1**	**N2**	**N3**	**N4**	**N5**	**N6**
Ω	30	150	270	30	150	210	90	270	330
active	8	8	5	5	5	5	6	6	4
non-active	9	42	44	2	4	1	3	3	4

Table 2: Groups of GLONASS and GPS satellites.

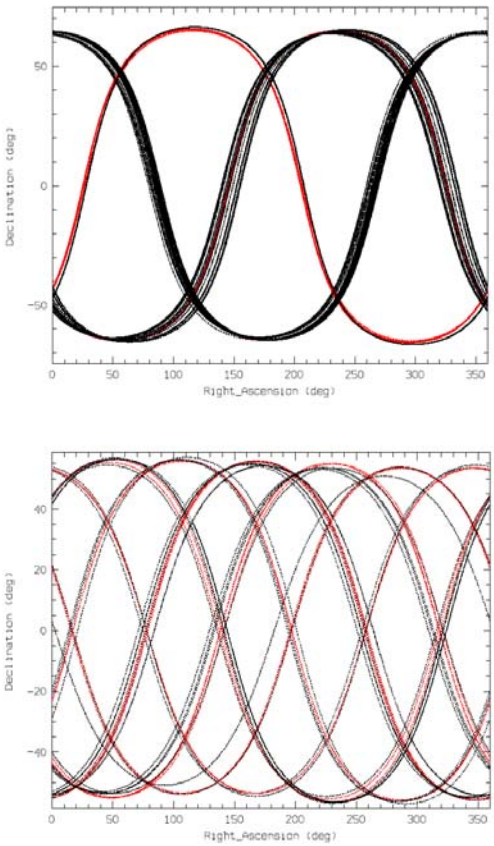

Figure 3: Tracks of all GLONASS (top) and GPS (bottom) satellites in a geocentric (α, δ)-system. Active satellites are in red and non-active satellites in black.

During the time between January 2010 and November 2010 on 44 nights 284 surveys were performed with the ESASDT. This corresponds to 3124 minutes (≈ 52 hours) of observations. Here one survey is defined as the observation of one field during 11 minutes, the time needed for the acquisition of 29 frames. A summary for all campaigns is given in Table 3. The last row includes the total observation time.

Group/Plane	N1	N2	N3	N4	N5	N6	G1	G2	G3
January	14	0	0	6	0	0	8	0	0
February	8	0	0	8	0	0	0	0	0
March	2	0	0	3	0	0	14	8	0
April	0	5	0	0	0	0	6	5	0
May	0	0	0	0	0	0	0	37	0
June	0	0	0	0	0	0	0	0	0
July	0	0	0	0	0	0	0	0	0
August	0	0	0	0	0	0	0	0	0
September	1	0	0	0	0	0	3	15	0
October	0	0	14	0	0	0	33	3	0
November	0	0	0	0	0	0	0	0	91
Time in min.	275	187	55	154	0	0	704	748	1001

Table 3: Number of surveys for each satellite group. The last row gives the total observation time.

IV. ANALYSIS AND RESULTS

No "new" object in a MEO orbit was found throughout 52 hours of MEO surveys. By "new object" we mean an object which could not be correlated with the existing orbit catalogues (in particular the USSTRATCOM TLE catalogue). In ESASDT GEO surveys we discover on average about one object every 45 minutes. The spatial density of catalogued objects in the region of the MEO navigation constellations is much lower than in GEO and thus we obviously expect a lower density for an associated debris population. It is worth mentioning that, on the other hand, all catalogued objects crossing any of the survey fields were detected, or in other words, there were no "no-shows".

The fact that we did not see a single unknown object in the surveys does not imply that there is no uncatalogued debris in MEO, but provides an upper boundary for the number of debris in the region covered by the survey. In the following we try to estimate the probability for a breakup event in 6 of the observed orbital planes of the GPS and GLONASS navigation constellations. As a baseline for this assessment we use the synthetic breakup population described in Section II.

The observed fields in (α, δ) correspond to regions in the (i, Ω) space as described in Figure 2. These regions in turn determine the number of objects of the hypothetical population that can be detected. The number is related to the volume defined by the section of the two-dimensional normal distribution of the population delimited by the FOV of the telescope. The integral of the cross section is easiest to calculate when the measurements are done at the point of maximum declination (culmination) or at the node of the observed orbit, e.g. for GPS satellites the culmination would be around 55 deg declination. In this case the calculation reduces to a one-dimensional integration over the interval delimited by the FOV.

A simplified representation of the coverage of the GLONASS G1 orbit plane by the surveys is given in Figure 4. The coordinates of the middle of the stripe indicate approximately the geocentric α, δ of the actually observed field. The length of the stripes denotes the total observation time of the single field expressed in number of equivalent fields. With the assumption of a 70 s dwell time, a 10 minutes survey on one field correspond to the equivalent of 8.5 fields along the orbit, and a stripe length of 8.5 x 0.7 deg ≈ 6 deg. During the survey campaign the same field was repeatedly observed at different times and on several nights. Therefore the indicated stripes in general have arcs longer than 6 deg. The blue dotted line shows the positions for an object in the nominal (average) orbital plane.

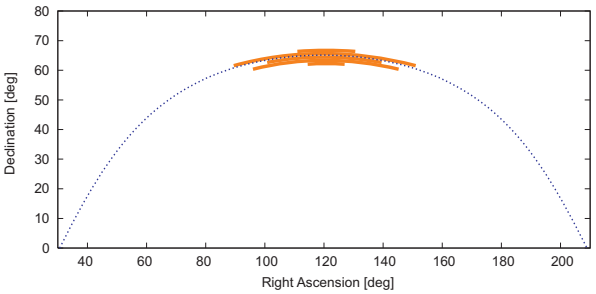

Figure 4: Simplified representation of the number of observed fields in the survey of the group G1.

Since the surveys do not cover the entire orbit of a hypothetical object it is only possible to make some statistical considerations. The statistical problem can be described as the classical distribution of k successes in a sequence of n independent yes/no experiments, each of which yields success with probability p. This problem is described by the binomial distribution. The probability p_k of getting k successes is given by:

$$p_k = \binom{n}{k} p^k (1-p)^{n-k} . \qquad (2)$$

The probability p for a single sampling experiment is given by the number of objects m in this orbit divided by the total number of fields in one inclination stripe along the entire orbit, i.e. by 360 deg / 0.7 deg = 514. For our surveys we have to set, $k = 0$, since no new object was found, n is the number of observed fields, and $m = 512p$ is the number of objects. Here we need to assume that the distribution of the survey fields along the orbit is random, which is a reasonable assumption because the time of observation during the night varied considerably and was arbitrarily chosen by the observer at the ESASDT. Furthermore in the following considerations we assume that at most one object per field can

be found. The assumption is justified by the fact that k is very small compared to n (or m<<512), consequently also p will be quite small and the probability to find two objects in the same field at the same time is almost vanishing.

The common estimator p' for the binomial distribution yields $p' = k/n = 0$. We thus determine a confidence interval $[p_l, p_u]$ with a lower limit p_l and an upper limit p_u around p'. For a 95% confidence level with $k = 0$, the lower limit is $p_l = 0$, while p_u is determined by the area of the distribution delimited by k. The unknown p_u for a confidence level of 95% id given by the inverse beta function:

$$p_u = \beta^{-1}(95\%, k+1, n) \cdot \tag{3}$$

In the following tables a normalization factor is applied to the observed number of fields to account for the fact that only a fraction of the hypothetical breakup population is sampled by a given survey field. For the surveys at the culmination the normalization factor depends only on the geocentric declination of the survey field, which corresponds to an inclination for the sampled orbital plane. Table 4, Table 5 and Table 6 summarize the number of observed fields and the estimated upper limit for the number of objects for a 95% confidence level for the groups N1, N2, and N3. The number of samples (fields) for the GPS orbital planes is not very high and the estimated upper limit for the number of objects is consequently quite large.

# Fields	Incl. [deg]	Norm.	Norm. # fields
180	53.6	0.12	21
# Objects			73

Table 4: Number of fields and maximum number of objects (95% confidence level) for the N1 group.

# Fields	Incl. [deg]	Norm.	Norm. # fields
43	53.6	0.12	5
# Objects			308

Table 5: Number of fields and maximum number of objects (95% confidence level) for the N2 group.

# Fields	Incl. [deg]	Norm.	Norm. # fields
42	54.3	0.16	7
26	53.6	0.12	3
34	52.2	0.04	1
Sum			11
# Objects			140

Table 6: Number of fields and maximum number of objects (95% confidence level) for the N3 group.

The number of observed fields and estimated upper limits of objects for the GLONASS G1, G2, and G3 orbital planes are given in Table 7, Table 8 and Table 9. For the G3 group the survey fields were not located close to the culmination because of visibility constraints. For these fields the normalization factor depends on not only on the geocentric declinations but also on the geocentric right ascension of the field. Each field corresponds to a specific orbital plane (i, Ω).

Table 9 indicates for every field (α, δ) the corresponding orbit (i, Ω) closest to the nominal GLONASS orbit among the orbits covered by the field. In fact survey fields cover a range of inclinations and nodes. While a field at the culmination covers the whole range of nodes of the population, in general a field covers only a reduced region in the (i, Ω)-space. The normalization factor is determined by evaluating the volume integral of the cross section of the two-dimensional normalized breakup population distribution with the FOV. Figure 5 gives a representation this distribution and the FOV cross section which is the region delimited by the two parallel planes. The orientation of the planes is related to (α, δ).

There were considerable more surveys performed for GLONASS orbital planes than for GPS ones and the inferred limits for the number of objects are thus lower. The upper limit for the G3 group is a surprisingly small number of 6 objects.

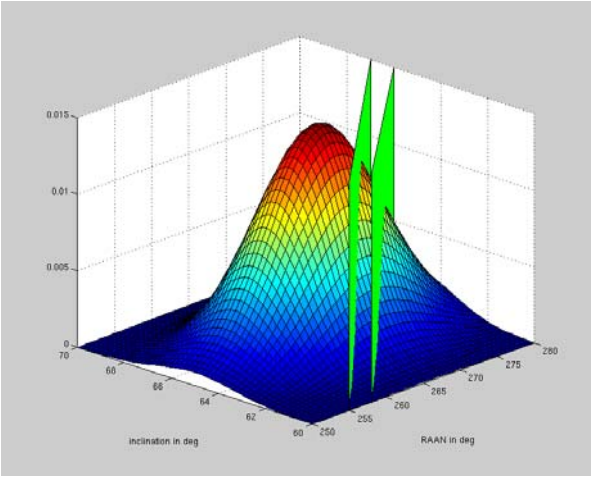

Figure 5: Two-dimensional normalized breakup population distribution of G3. The region sampled by a specific FOV is the region delimited by the two parallel planes.

# Fields	Incl. [deg]	Norm.	Norm. # fields
17	62.4	0.07	1
77	63.1	0.12	9
60	63.8	0.16	9
94	64.5	0.17	16
34	65.2	0.16	5
Sum			40
# Objects			38

Table 7: Number of fields and maximum number of objects (95% confidence level) for the G1 group.

# Fields	Incl. [deg]	Norm.	Norm. # fields
377	64.5	0.17	65
94	63.1	0.12	11
Sum			76
# Objects			20

Table 8: Number of fields and maximum number of objects (95% confidence level) for the G2 group.

# Fields	RA [deg]	DE [deg]	Ω [°]	Incl. [deg]	Norm.	Norm. # fields
26	270.5	6.92	266.6	64.5	0.18	5
60	290.5	40.1	266.6	64.5	0.24	15
77	307.0	53.63	266.6	64.5	0.35	27
68	283.5	30.63	266.6	64.4	0.21	14
188	293.5	43.2	266.6	64.4	0.26	49
137	83.25	7.08	266.6	64.5	0.17	24
120	311.75	55.58	266.6	64.4	0.39	47
51	315.0	57.87	266.6	64.4	0.42	22
51	78.5	17.25	266.6	64.4	0.18	9
103	301.75	50.08	266.6	64.4	0.32	33
Sum						244
# Obj.						6

Table 9: Number of fields and maximum number of objects (95% confidence level) for the G3 group.

If we recall the fragment distribution of the breakup population (Figure 1), we expect around 200 objects with a size larger than the detection limit for the ESASDT, which is about 20cm. We may thus exclude a breakup event of the type modeled by our synthetic population with a 95% confidence in the three orbital planes of the GLONASS constellation and in two of the three analyzed GPS planes. There is no observational evidence for a breakup in the remaining GPS planes but the observation data is too limited to exclude such an event.

V. SUMMARY AND CONCLUSIONS

The ESA MEO surveys constitute in fact the first attempt to observationally characterize the small-size debris environment in MEO.

Experimental MEO observation campaigns were conducted with the 1-meter ESA Space Debris Telescope (ESASDT) on Tenerife during the year 2010. The surveys covered three orbital planes of the GPS navigation satellite constellation and 3 orbital planes of the GLONASS constellation.

No "new" object was found in the mentioned orbital planes throughout 52 hours of MEO surveys (new with respect to the USSTRATCOM TLE catalogue). (The same number of surveys in GEO would result in approximately 70 new objects.) There is thus no direct observational evidence for unknown debris in the mentioned orbital planes, but given the very limited observation sample we can obviously not exclude debris in this region.

A synthetic breakup population described in analytical form was used to derive statistical upper limits for the number of objects in the surveyed orbital planes. These limits range from 6 to 308 objects depending on the number of surveys for a given orbital plane.

A breakup event of a large object would have produced about 200 observable objects larger than 20cm. The main result of the surveys is thus that with a 95% confidence no breakup of a large object has occurred in 5 out of the 6 analyzed MEO navigation satellite orbital planes.

The results are based on a limited observation sample of 52 hours. A considerable larger sample is required to characterize the small-size debris environment and to exclude breakup events in the entire MEO navigation constellation region.

VI. REFERENCES

[1] Schildknecht, T., W. Flury, C. Früh, J. Herzog, A. Hinze, A. Vananti, Using Optical Observations to Survey, Track, and Characterize Small-Size Objects at High Altitudes, 28th International Symposium on Space Technology and Science, June 5-12, 2011, Okinawa, Japan, 2011.

[2] Oswald, M., Wegener, P., Stabroth, S., Wiedemann, C., Rosebrock, J., Martin, C., The Master 2005 Model, Proceedings of the 4th European Conference on Space Debris (ESA SP-587), 18-20 April 2005, ESA/ESOC, Darmstadt, Germany, p.235, 2005.

[3] Schildknecht, T., T. Flohrer, A. Vananti, Optical Surveys for Space Debris in MEO, IAC-09-A6.1.4, 60th International Astronautical Congress, October 12 – 18, Daejeon, Republic of Korea, 2009.

[4] Pardini, C., L. Anselmo, 'Dynamical evolution of debris clouds in geosynchronous orbit', Advances in Space Research 35, pp. 1303-1312, 2005

[5] Donath, Th., T. Schildknecht, P. Brousse, J. Laycock, T. Michal, P. Ameline, L. Leushacke, 'Detailed Assessment of a European Space Surveillance System', Final Report ESA/ESOC Contract 18574/04/D/HK(SC), 2005.